Detrapping of tungsten nanoparticles in a direct-current argon glow discharge

Lénaïc Couëdel, Kishor Kumar K., C. Arnas

Detrapping of tungsten nanoparticles in a direct-current argon glow discharge

L. Couëdel,[a] Kishor Kumar K.,[b] and C. Arnas

CNRS, Aix-Marseille Université, Laboratoire de Physique des Interactions Ioniques et Moléculaires, 13397 Marseille, France.

Nanoparticles are grown from the sputtering of a tungsten cathode in a direct current argon glow discharge. Laser light scattering of a vertical laser sheet going through the plasma reveals that the dust particle cloud is compressed and pushed towards the anode during the discharge. Scanning electron microscopy images of substrates exposed to the plasma for given durations show that dust particles are continuously falling down on the anode during the discharge. These observations are explained by the fact that the electrostatic force at the negative glow-anode sheath boundary cannot balance the ion drag, gravity and thermophoresis forces for particles of more than a few tens of nanometres in diameter.

PACS numbers: 52.27.Lw

[a] Electronic mail: lenaic.couedel@univ-amu.fr

[b] Current address:Center for Plasma-Materials Interactions, 216 Talbot Laboratory, 104 S Wright Street, University of Illinois at Urbana-Champaign, 61801 Illinois, USA

I. INTRODUCTION

Dusty or complex plasmas are partially ionised gas which contain solid dust particles[1,2]. These particles acquire an electric charge due to their interactions with the surrounding ions and electrons. In laboratory experiments, particles can be either injected or grown directly inside the plasma. For example, they can be produced in astrophysical plasmas[3], in industrial plasma processing reactors[4], in tokamaks from the physical and chemical erosion of the wall[5], etc.

The production of nanoparticles in low pressure, low temperature plasmas have been extensively studied. It was shown that the particles can be generated following specific chemical reactions up to the formation of solid particles. In particular the growth of nanoparticles in radio-frequency (rf) discharges using reactive gases[6–12] or by sputtering of a cathode[13] was carefully investigated. In such systems, it was shown that the dust particles are confined in the plasma and that their growth occurs in cycles[11,12,14]. In particular, the growth of new particles can occur when the previous dust cloud is expelled from the central region of the plasma so that the conditions are again favourable to nucleation and growth[12,14]. The dust cloud can be expelled towards the edges of the discharge when the dust density is too high and/or the particles too big so that the repulsion forces become larger than the confining forces[15–17]. The particles can also fall on the electrode when they reach a critical size and their weight cannot be balanced by the confining forces. In rf discharges this is normally the case when the particles reach a few tens of micrometers in diameter[18].

The growth of nanoparticles by cathode sputtering in direct-current (dc) glow discharges have also been reported[19–22]. Using an aluminium cathode, it was shown that the spatial profile of the particle cloud was very sensitive to discharge parameters, especially the applied voltage[19]. Moreover, studies on the production of nanoparticles in dc discharges by sputtering of a graphite cathode have shown a strong coupling between plasma and discharge parameters and, the particle growth kinetics[21]. In a recent study in which we used a tungsten cathode in similar condition as in Ref.[21], we showed that the evolution of the dust particle size distribution (PSD) was quite unusual[22,23]:

- small particles were always observed indicating constant nucleation,
- growth by agglomeration did not seem to saturate as reported for carbon nanoparticles,

- there was a strong dispersion in the appearance time of the second dust particle generation.

Furthermore, the evolution of the discharge and plasma parameters were a competition between the influence of the cathode surface state (tungsten oxidation) and the influence of the charging process of the nanoparticles[22]. The latter was evident only after a few hundreds of seconds. However, the motion of the dust particle cloud was not investigated and it was supposed that the dust particles remained confined in the plasma until the discharge was switched off.

In this article, we investigated the behaviour of a nanoparticle cloud grown by sputtering of a tungsten cathode in a dc argon glow discharge with similar conditions to those of Refs.[21,22]. The aim of these investigations was to link the previously reported evolution of the PSDs to the dust cloud motion. For this purpose, laser light scattering of a vertical laser sheet going through the plasma revealed that the dust particle cloud was compressed and pushed towards the anode during the discharge. By exposing substrates to the plasma on the anode side of the discharge, it was also found that dust particles were continuously falling on the anode. This result is explained by the inhomogeneous nature of the dc glow discharge. Due to the low electron temperature and the weak electric field in the anode sheath, the confining electric force is too weak to balance the ion drag, gravity and thermophoretic forces for particles of more than a few tens of nanometres in diameter.

II. EXPERIMENTAL SET-UP

A detailed description of the experimental set-up is given in Ref.[22]. The tungsten nanoparticles were grown in a dc argon glow discharge initiated between a ∼10 cm diameter tungsten cathode and a stainless-steal grounded anode. The inter-electrode distance was 10 cm. The cathode was enclosed in an insulating ceramic holder so that only one side was exposed to the plasma. Two glass half-cylinders were used to confine the plasma. A 1 cm gap was kept between them for optical studies (see Fig.1). A static argon pressure of 0.6 mbar (no gas flow) was set during the experiments. The electrode assembly was contained in a cylindrical vacuum chamber of 30 cm diameter and 40 cm length. An oil diffusion pump achieved a base pressure of $\leq 10^{-6}$ mbar. A manually operated gate valve was used to isolate the chamber from the oil diffusion pump during experiments.

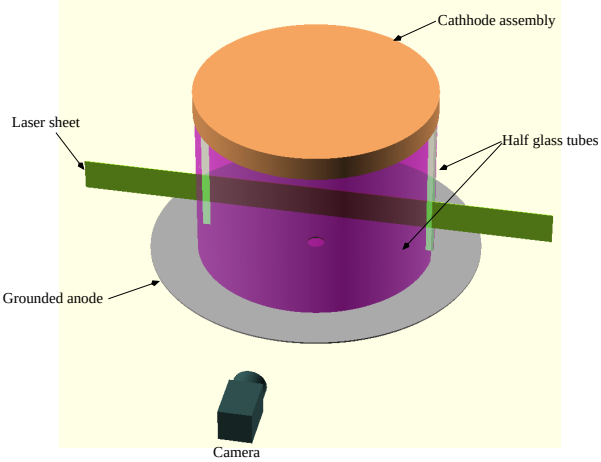

FIG. 1. (Colour online) Schematic of the cathode assembly

A regulated power supply (Sefelec HT15A, 1 kV, 300 mA) was used to bias the cathode. The discharge current density was kept at a constant value (0.53 mA·cm^{-2}). The current variations were less than 0.05 %. The discharge parameters were such that the plasma mainly consisted of a negative glow. The discharge voltage was the free parameter whose time evolution was acquired during the discharge. Under the chosen operating conditions, the cathode was sputtered and tungsten nanoparticles were grown. More details about the evolution of discharge parameters during the nanoparticle growth are given in Ref.[22].

In order to image the dust particle cloud and to measure the evolution of the PSD during the discharge, two diagnostics have been used:

A. Laser light scattering

A 2 cm height vertical laser sheet (40 mW, wavelength $\lambda = 532$ nm) was passing through the electrode assembly in the gap between the half-cylinders (see Fig.1). The scattered light by the dust particles was recorded at 90° by a CCD camera (BASLER ACE acA1300-60gm). A low frame rate of 1 frame per second and a long exposure time of 0.5 s were used in order to detect the weak scattered light signal. The position of the laser sheet between the electrode could be chosen at the time of the experiment. A bandpass filter centred on the laser wavelength was placed in front of the camera in order to minimise the recorded plasma light.

B. Scanning electron microscopy

The anode disc had a 1.6 cm diameter hole at the centre through which the tungsten nanoparticles produced during the discharge were collected. Stainless steel foils, mounted on a holder were used as substrates for collecting the dust. The substrate holder could be manipulated from one of the axial ports of the chamber, such that each of them could be positioned under the hole in the anode. Dust particles were then analysed ex-situ using a scanning electron microscope.

Two methods of collection have been used:

- (i) The substrate holder was moved under the anode so that successive substrates were exposed to the plasma only during a given time interval.
- (ii) The substrate saw the end of the discharge. Note that in this case, the substrate could be or not exposed to to the plasma during the whole discharge duration.

III. RESULTS

A. Laser light scattering

During the experiment, the vertical laser sheet was grazing the anode. In Fig.2-(a), snapshots of the video at different instants after the plasma ignition are presented. The time evolutions of the recorded light signal at different position above the anode are also shown as well as the evolution of the cathode voltage V_c (Fig.2-(b)). The light recorded above the laser sheet (position 2.33 cm and 2.14 cm) represents the residual plasma light. This allowed us to discriminate the scattered light from the plasma emission. During the first $\sim$150 s, no particles could be detected in the video images. However, it is known from the cathode voltage evolution (Fig.2-(b)) that dust particles were already present between the electrode (for more details, see Ref.[22]). It probably indicates that either the dust particles were not located above the anode or they were too small and/or their density was too low to be detectable through laser light scattering. From t $\sim$150 s, scattered light could be detected at the top edge of the laser sheet. Note that this appearance time varied of $\sim$30 s from one experiment to the other as the dust particle growth kinetics is very sensitive to initial conditions. This behaviour was also reported in rf discharges in which particles were growing

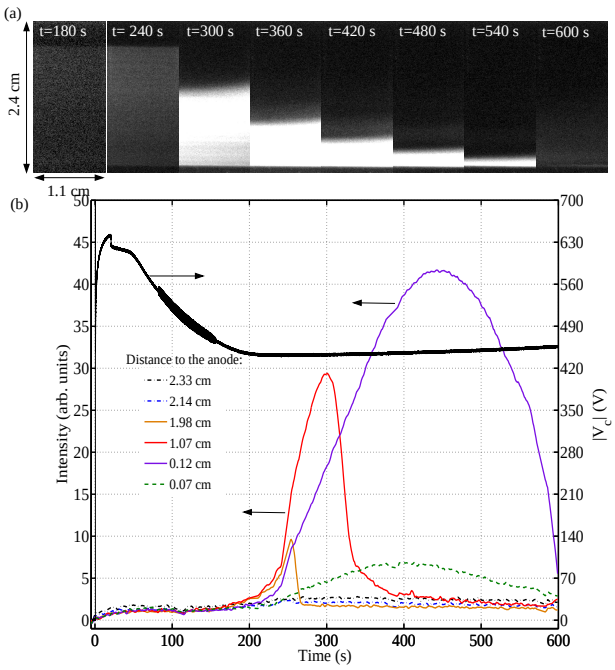

FIG. 2. (Colour online) (a) Snapshots of the video. The laser sheet was grazing the anode. At $t = 180$ s, luminosity and contrast were enhanced compared to the other images. (b) Evolution of the cathode voltage as a function of time (Right vertical-axis, black plain line) and evolution of the recorded scattered light intensities at different distance from the anode (Left vertical-axis). The two highest positions (2.33 cm and 2.14 cm) show intensities recorded outside the laser sheet and show only the residual plasma light. The lowest position (0.07 cm) shows the light intensity recorded in the anode sheath.

from the sputtering of a polymer layer[24]. At t$\sim$180 s, a dust cloud could be observed across the whole laser sheet except in the anode sheath (a $\sim$0.15 cm wide region above the anode). Up to t$\sim$250 s, the scattered light signal was increasing across the whole laser sheet. This indicated that the dust particle cloud was getting denser and/or the particles were getting bigger. In Fig.2-(a) (snapshot at $t = 240$ s), the dust cloud seems to be homogeneous. This is also supported by the recorded scattered light intensities at different height in the laser sheet which have almost the same values.

For $t \gtrsim 250$ s, the scattered light signal at the top of the laser sheet decreased strongly while the signal in the middle and at the bottom of the laser sheet (except in the anode sheath) were still strongly growing. From the snapshots of Fig.2-(a), it is clear that the dust cloud was compressed towards the anode. After $t \gtrsim 300$ s, the dust cloud occupied only half

of the laser sheet width and was shrinking continuously. It should however be noted that a faint scattered light signal revealed the presence of a second NP cloud above the main dust cloud (Fig.2-(a) snapshots at $t = 300$ s, $t = 360$ s, $t = 420$ s, $t = 480$ s and, $t = 540$ s). Both clouds were separated by a non-emissive layer. From $t \sim$580 s, only the second dust cloud was visible above the anode. It should also be noted that from $t \sim$250 s, the intensity recorded inside the anode sheath was systematically above the residual plasma light signals (see Fig.2-(b), curve at 0.07cm). It is not clear that this was due to particle falling inside the sheath or due to an anode glow.

B. Scanning electron microscopy

In a previous study[22], the dust particles were collected at the end of the discharge on substrates exposed to the plasma for the entire experiment duration. In the present study, the samples were exposed to the plasma during a given time interval. Consequently, only the particles which were expelled from the plasma (i.e. falling on the anode) during this time lapse were collected. In Fig.3, PSDs of particles collected at different moments during two different discharges are shown. For example, in Fig.3(a), it can be seen that dust particles were collected for all chosen time intervals. The SEM image in the inset of Fig.3(a) shows particles which fell on the anode from $t = 200$ s to $t = 300$ s. Moreover, the later the substrate is exposed the bigger the particles. A striking difference with the previous study of Kishor Kumar K. et al.[22] was that even for long time, PSDs remained here mono-modal. It was indeed previously shown that for long discharge duration ($t \gtrsim$200 s) the PSDs were bi-modal. However, in the present case, PSDs are bimodal only when the plasma was switched off (see Sec.II B method (ii)). For example, the inset of Fig.3-(b) shows the bi-modal distribution obtained at the end of a 500 s plasma. These PSDs were similar to the distributions already reported in Ref.[22]. Laser light scattering explains this results: the smallest particles were confined in the negative glow above the cloud of big particles (the dim cloud above the bright cloud) and they could be collected only after the discharge was switched off.

It should be noted that from one experiment to the other, the size and the number of the collected dust particles were not exactly the same. This observation could be explained by the fact that the particle growth kinetics is very sensitive to the initial condition as previously

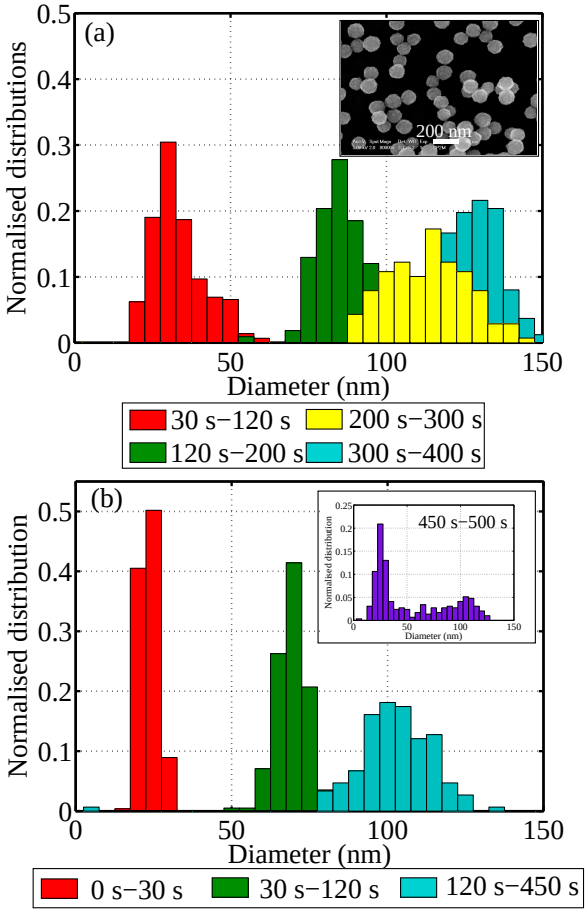

FIG. 3. (Coulour online) Normalised PSDs of particles collected on substrates exposed to the plasma at different times after ignition. (a) and (b) are two different experiments with the same discharge parameters. Inset of (a): SEM image of particles collected on a substrate exposed to the plasma from 200 s to 300 s. Inset of (b): Normalised PSD of particles collected after the discharge was switched of at t =500 s.

stated. However, it was possible to get a rough estimate of the flux of dust particle falling on the anode. Depending on the experiment, the number of particles collected on a substrate exposed to the plasma during 100 s was $N_p = 1 - 100$ μm^{-2} giving a flux of falling particles $\Gamma_p \sim 10^6 - 10^8$ cm^{-2}·s^{-1}.

IV. DISCUSSION

In the previous section, it was shown that nanometre size particles were falling continuously on the anode at a rate $\Gamma_p \sim 10^6 - 10^8$ cm^{-2}·s^{-1}. This results might be surprising as

it is believed that, as in rf discharges, growing dust particles remain confined in the inter-electrode space until they are too large (usually a few tens of micrometers) or their density too high for the confining forces to balance the repulsion forces[11,15–18,25].

In order to understand why dust particles are constantly falling on the anode during their growth, the forces acting on them must be estimated. Let us first consider the force pushing the particles towards the anode. (a) The gravity force $F_g = (4/3)\pi r_d^3 \rho g$ where r_d is the radius of the dust particle, g the gravitational constant and ρ the mass density. In our experimental conditions, considering pure tungsten particles, the gravity force were for $r_d = 15$ nm and $r_d = 50$ nm, $|F_g| = 2.5 \cdot 10^{-18}$ N and $|F_g| = 9 \cdot 10^{-17}$ N, respectively. (b) During the discharge, the cathode was heated up to ∼100°C while the anode stayed at room temperature[21,26]. The dust particle were then subject to a downward thermophoretic force[27–29] [30]..

$$F_t = -(32/15) r_d^2 k_{tr} / v_{Tn} \nabla T$$

where $v_{Tn} = \sqrt{8 k_B T_n / (\pi m_n)}$ is the neutral thermal velocity with k_B the Boltzmann constant, T_n the neutral atom temperature and m_n their mass. ∇T is the temperature gradient and the thermal conductivity $k_{tr} = (15 k_B/(4m_n))\mu_{ref}(T/T_{ref})^{\nu}$ with $\mu_{ref} = 2.117 \cdot 10^{-5}$ Pa·s for argon, $T_{ref} = 273$ K and $\nu = 0.81$[31]. In our discharge, considering a temperature gradient $\nabla T = 7$ K/cm, the thermophoretic forces were $|F_t| = 1.5 \cdot 10^{-17}$ N and $|F_t| = 1.7 \cdot 10^{-16}$ N for $r_d = 15$ nm and $r_d = 50$ nm, respectively. Note that during our experiments, the motion of the dust cloud and dust collection were performed close to the discharge axis far from the glass wall. Moreover, no convective motion of the dust particle cloud was observed on the video. Consequently, the gas creep effect induced by the thermal gradient was neglected in our force estimate. However, close to the edge of the discharge, this effect might be of great importance as it has been proven to be very efficient to induce strong convective dust motion[32–34].

In order to estimate the magnitude of forces due to the plasma, it is necessary to have a good approximation of the potential, electric field, electron and ion densities at the boundary between the negative glow and the anode sheath. The structure of a dc glow discharge is stratified and the plasma parameters are inhomogeneous along the discharge axis:

- In the negative glow the electron distribution function is composed of three electron populations[35–37]: the fast electrons (secondary electrons emitted by the cathode surface

and accelerated in the cathode fall region), the intermediate electrons (which ensure the current continuity), and the cold electrons produced by ionisation (with a temperature T_e ∼0.1 eV). The density of the cold electrons is orders of magnitude higher than the densities of intermediate and fast electrons. Modelling performed for our discharge geometry and similar discharge parameters showed that in the negative glow, the contribution of fast and intermediate electrons to the dust particle charging is limited[36]. Consequently, only cold electrons will be considered in the following. Langmuir probe measurements near the cathode[36] have shown that the plasma density in the negative glow is $n \sim 10^{10}$ cm^{-3} . The plasma density quickly drops when getting closer to the anode.[38]. A density $n \sim 10^9$ cm^{-3} is assumed at the anode sheath boundary.

- In the negative glow region, the electric field is weak[39]. Close to the sheath boundary, the plasma potential is positive with respect to the anode potential for high current density[37]. Consequently, the electric field tends to confine negatively charged particles in the inter-electrode space. However, the voltage drop in the anode sheath is around two order of magnitude lower that in the cathode sheath. Hybrid and PIC simulations have shown that the maximum electric field in the anode sheath is 10-20 V/cm and around 1 V/cm at the negative glow anode sheath boundary[38].

The dust density n_d in the discharge is unknown but typical values for dust particles grown from the sputtering of an electrode in plasmas are in the range[13,40,41]: $10^4 - 10^8$ cm^{-3}. Using the Orbital Motion Limited theory[42–44] and the quasi-neutrality condition $n_i = n_e + Z_d n_d$ where $n_{i(e)}$ is the ion (electron) density, one can calculate the dust particle charge number Z_d. Depending on the dust density, one obtains $Z_d = [-5,\ -4]$ and $Z_d = [-13,\ -7]$ for $r_d = 15$ nm and $r_d = 50$ nm, respectively. At the anode sheath boundary, two forces tend to push the particles: the ion drag which tends to push the particles on the anode and, the electric force which confines them in the plasma. The ion drag force is[45]:

$$
\begin{aligned}
F_{di} &= F_{di}^{coll} + F_{di}^{coul} \\
F_{di}^{coll} &= \pi n_i m_i v_i v_s b_c^2 \\
F_{di}^{coul} &= 4\pi n_i m_i v_i v_s b_{\pi/2}^2 \Gamma_c
\end{aligned}
$$

where m_i is the ion mass, $v_i = \mu_i \mathrm{E}$ the ion drift velocity. μ_i is the ion mobility, E the electric field, $v_s = \sqrt{v_{Ti}^2 + v_i^2}$ with the ion thermal velocity $v_{Ti} = v_{Tn}$. $b_c = r_d \cdot (1 -$

$2e^2 Z_d/(4\pi\epsilon_0 r_d m_i v_s^2))^{1/2}$ is the radius of closest approach, $b_{\pi/2} = e^2 Z_d/(4\pi\epsilon_0 m_i v_s^2)$ and, the Coulomb logarithm: $\Gamma_c = 0.5 \cdot \ln((\lambda_{De}^2 + b_{\pi/2}^2)/(b_c^2 + b_{\pi/2}^2))$ where λ_{De} is the electron Debye length. Depending on the strength of the electric field, the ion drag force was in the range $F_{di} \sim 10^{-19} - 10^{-18}$ N for 15 nm radius. For 50 nm radius, the ion drag force was in the range $F_{di} \sim 10^{-18} - 10^{-17}$ N. In both cases it is negligible compared to the combined influence of the gravity and thermophoretic forces. However, the upward force due to the anode sheath electric field is $F_E \sim 5 \cdot 10^{-17} - 5 \cdot 10^{-16}$ N for $r_d = 15$ nm and $F_E \sim 2 \cdot 10^{-16} - 2 \cdot 10^{-15}$ N for $r_d = 50$ nm.

By balancing the different forces, one can see that the 50 nm radius dust particles can be pushed on the anode by the gravity and the thermophoretic force while the 15 nm radius ones can be confined in the negative glow. In our force estimate, the influence of photoemission[46] which charges the particle positively, i.e. decreases their negative charges, and, the influence of a high dust density which can drastically affect the plasma parameters were neglected. However, it was observed experimentally from SEM images that growing dust particles were falling on the anode at all times. Nevertheless, laser light scattering showed that even if the dust cloud was compressed toward the anode, it took hundreds of seconds before it disappeared completely from the plasma. This indicates that the force pushing down the dust particles were of the same order of magnitude as the confining one, as our force estimate shows. Furthermore, small particles were always collected on the substrate at the end of a discharge as shown here and in our previous studies[22]. On the contrary, they were only collected at the beginning of the discharge for substrates exposed to the plasma at the beginning of the experiments (see Sec.II B, method (i)). These results indicate that small dust particles were always produced in the plasma and located above the big particles (first generation), these last ones being expelled little by little. As the big particles are evacuated, favourable conditions for a constant formation occur in the upper part of the negative glow.

V. CONCLUSION

In this article, it was shown that in dc argon glow discharges dust nanoparticles were pushed towards the anode located at the bottom of the discharge set-up and could be detrapped and fell on it. Due to a low electron temperature and weak electric field in the anode sheath, the electric force cannot balance the ion drag, thermophoretic and the gravity

forces as soon as the particle size reach a few tens of nanometres. The previous observation of $r_d \sim 15$ nm particles when the discharge was operated with different durations[22] can be explained by the constant nucleation and growth of particles in the upper part of the discharge (cathode side). Indeed, as the big particles are evacuated, favourable condition for nucleation and growth might occur at all time at the top of the negative glow.

ACKNOWLEDGMENTS

This work was supported by ANR contract (n° ANR-09-BLAN-0070-01-CRWTH) and by Euratom/CEA association in the framework of FR-FCM and EFDA.

REFERENCES

[1]A. Bouchoule, *Dusty Plasmas: Physics, Chemistry and Technological impacts in Plasma Processing* (Wiley, New York, 1999).

[2]G. E. Morfill and A. V. Ivlev, Rev. Mod. Phys. **81**, 1353 (2009).

[3]C. K. Goertz and G. Morfill, Icarus **53**, 219 (1983).

C. J. Mitchell, M. Horanyi, O. Havnes, and C. C. Porco, Science **311**, 1587 (2006).

[4]G. S. Selwyn, J. Singh, and R. S. Bennett, J. Vac. Sci. Technol. A **7**, 2758 (1989).

L. Boufendi, J. Gaudin, S. Huet, G. Viera, and M. Dudemaine, Appl. Phys. Lett. **79**, 4301 (2001).

D. Vollath, J. Nanopart. Res. **10**, 39 (2008).

[5]J. Winter, Plasma Phys. Control. Fus. **40**, 1201 (1998).

J. Sharpe, D. Petti, and H.-W. Bartels, Fusion Eng. Des. **6364**, 153 .

C. Arnas, C. Pardanaud, C. Martin, P. Roubin, G. D. Temmerman, and G. Counsell, J. Nucl. Mat. **401**, 130 (2010).

[6]A. Bouchoule and L. Boufendi, Plasma Sources Sci. Technol. **2**, 204 (1993).

[7]C. Hollenstein, Plasma Phys. Control. Fus. **42**, R93 (2000).

[8]C. Hollenstein, J. L. Dorier, J. Dutta, L. Sansonnens, and A. A. Howling, Plasma Sources Sci. Technol. **3**, 278 (1994),.

[9]Y. Watanabe, J. Phys. D: Appl. Phys. **39**, R329 (2006).

[10]C. Deschenaux, A. Affolter, D. Magni, C. Hollenstein, and P. Fayet, J. Phys. D: Appl. Phys. **32**, 1876 (1999).

[11]S. Hong, J. Berndt, and J. Winter, Plasma Sources Sci. Technol. **12**, 46 (2003).

[12]M. Hundt, P. Sadler, I. Levchenko, M. Wolter, H. Kersten, and K. K. Ostrikov, J. Appl. Phys. **109**, 123305 (2011),.

[13]D. Samsonov and J. Goree, J. Vac. Sci. Technol. A **17**, 2835 (1999).

[14]M. Cavarroc, M. Mikikian, Y. Tessier, and L. Boufendi, Phys. Rev. Lett. **100**, 045001 (2008).

[15]A. A. Howling, C. Hollenstein, and P. Paris, Appl. Phys. Lett. **59**, 1409 (1991).

[16]P. R. i Cabarrocas, P. Gay, and A. Hadjadj, J. Vac. Sci. Technol. A **14**, 655 (1996).

[17]F. Greiner, J. Carstensen, N. Khler, I. Pilch, H. Ketelsen, S. Knist, and A. Piel, Plasma Sources Sci. Technol. **21**, 065005 (2012),.

[18]T. Nitter, Plasma Sources Sci. and Technol. **5**, 93 (1996).

[19]G. M. Jellum and D. B. Graves, J. Appl. Phys. **67**, 6490 (1990).

[20]C. Arnas, A. Mouberi, K. Hassouni, A. Michau, G. Lombardi, X. Bonnin, F. Bénédic, and B. Pégourié, J. Nucl. Mat. **390-391**, 140 (2009).

[21]C. Arnas, A. Michau, G. Lombardi, L. Couëdel, and K. K. Kumar, Phys. Plasmas **20**, 013705 (2013).

[22]Kishor Kumar K., L. Couëdel, and C. Arnas, Phys. Plasmas **20**, 043707 (2013).

[23]Kishor Kumar K., L. Couëdel and C. Arnas, J. Plasma Phys. **80**, 849 (2014).

[24]M. Mikikian, M. Cavarroc, L. Couëdel, and L. Boufendi, Phys. Plasmas **13**, 092103 (2006).

[25]J. H. Chu, J.-B. Du, and L. I, J. Phys. D: Appl. Phys. **27**, 296 (1994).

[26]C. Arnas and A. A. Mouberi, J. Appl. Phys. **105**, 063301 (2009).

[27]Z. Li and H. Wang, Phys. Rev. E **70**, 021205 (2004).

[28]L. Waldmann, Z. Naturforsch **14a**, 589 (1959).

[29]H. Rothermel, T. Hagl, G. E. Morfill, M. H. Thoma, and H. Thomas, Phys. Rev. Lett. **89**, 175001 (2002).

[30]The thermophoretic force expression used by Rothermel et al.[29] is almost the same as the original expression derived by Waldmann[28], the difference being in the multiplicative coefficient, and gives the same result within experimental errorbars ($\sim 30\%$).

[31]M. A. Gallis, D. J. Rader, and J. R. Torczynski, Aerosol Sci. Technol. **36**, 1099 (2002).

[32]S. Mitic, R. Sütterlin, A. V. I. H. Höfner, M. H. Thoma, S. Zhdanov, and G. E. Morfill, Phys. Rev. Lett. **101**, 235001 (2008).

[33]M. Schwabe, M. Rubin-Zuzic, S. Zhdanov, A. V. Ivlev, H. M. Thomas, and G. E. Morfill, Phys. Rev. Lett. **102**, 255005 (2009).

[34]M. Schwabe, L.-J. Hou, S. Zhdanov, A. V. Ivlev, H. M. Thomas, and G. E. Morfill, New J. Phys. **13**, 083034 (2011).

[35]V. I. Kolobov and L. D. Tsendin, Phys. Rev. A **46**, 7837 (1992).

[36]A. Michau, G. Lombardi, L. Colina Delacqua, M. Redolfi, C. Arnas, P. Jestin, X. Bonnin, and K. Hassouni, Plasma Chem. Plasma Process. **32**, 451 (2012).

[37]L. D. Tsendin, Plasma Sources Sci. Technol. **20**, 055011 (2011).

[38]Z. Donkó, P. Hartmann, and K. Kutasi, Plasma Sources Sci. Technol. **15**, 178 (2006).

[39]J. D. Cobine, *Gaseous Conductors: Theory and Engineering Applications* (Dover Publications, New York, 1958).

[40]G. M. Jellum and D. B. Graves, Applied Physics Letters **57**, 2077 (1990).

[41]A. Zeinert, C. Arnas, C. Dominique, and A. Mouberi, J. Vac. Sci. Technol. A **26**, 1450 (2008).

[42]J. E. Allen, Physica Scripta **45**, 497 (1992).

[43]C. Cui and J. Goree, IEEE Trans. Plasma Sci. **22**, 151 (1994).

[44]T. Matsoukas and M. Russell, Phys. Rev. E **55**, 991 (1997).

[45]M. S. Barnes, J. H. Keller, J. C. Forster, J. A. O'Neill, and D. K. Coultas, Phys. Rev. Lett. **68**, 313 (1992).

[46]P. K. Shukla and A. A. Mamun, *Introduction to dusty plasma* (IOP Publishing, Bristol, 2002).